ELSEVIER

Biochimica et Biophysica Acta 1565 (2002) 308–317

BIOCHIMICA ET BIOPHYSICA ACTA

BBA

www.bba-direct.com

Review

The structure of bacterial outer membrane proteins

Georg E. Schulz *

Institut für Organische Chemie und Biochemie, Albert-Ludwigs-Universität, Albertstr. 21, Freiburg im Breisgau 79104, Germany

Received 19 February 2002; received in revised form 26 April 2002; accepted 26 April 2002

Abstract

Integral membrane proteins come in two types, α-helical and β-barrel proteins. In both types, all hydrogen bonding donors and acceptors of the polypeptide backbone are completely compensated and buried while nonpolar side chains point to the membrane. The α-helical type is more abundant and occurs in cytoplasmic (or inner) membranes, whereas the β-barrels are known from outer membranes of bacteria. The β-barrel construction is described by the number of strands and the shear number, which is a measure for the inclination angle of the β-strands against the barrel axis. The common right-handed β-twist requires shear numbers slightly larger than the number of strands. Membrane protein β-barrels contain between 8 and 22 β-strands and have a simple topology that is probably enforced by the folding process. The smallest barrels form inverse micelles and work as enzymes or they bind to other macromolecules. The medium-range barrels form more or less specific pores for nutrient uptake, whereas the largest barrels occur in active Fe^{2+} transporters. The β-barrels are suitable objects for channel engineering, because the structures are simple and because many of these proteins can be produced into inclusion bodies and recovered therefrom in the exact native conformation.

Keywords: β-Barrel; β-Helix; β-Twist; Chainfold topology; Channel engineering; Shear number

1. Introduction

When searching through a recent set of protein sequences derived from genomic DNA sequences, it became evident that about 20% of all proteins are located in membranes [1]. This percentage was deduced from a search for transmembrane α-helices with a computerized prediction system, the results of which are known to come with a high confidence level. Such helices can be recognized by a continuous stretch of 20–30 nonpolar residues with a predominance of aliphatic side chains at the center and aromatic residues at both ends [2]. In an α-helix, the main chain amides are all locally complemented, so that the surface contacting the nonpolar membrane interior is exclusively formed by the nonpolar side chains. This explains the usefulness of an α-helix as a membrane-crossing element. Since the helix orientation can be deduced from the charge patterns of the inter-helical segments (positive inside and negative outside the cell), the so-called topologies of all these α-helical membrane proteins can be assessed from the sequence.

The presence of additional β-sheets in these proteins is discussed, but it cannot be expected that the membrane is faced by a mixture of α-helices and β-sheets, because the main chain hydrogen bond donors and acceptors at the sheet edges cannot be complemented by those of α-helices. This amide saturation problem at the edge strands of a transmembrane β-sheet can be abolished, however, if both edges associate to form a barrel. Since all amide hydrogen bond donors and acceptors are complemented, a β-barrel can face the nonpolar interior of the membrane if its outer surface is coated with nonpolar side chains. Such barrels occur indeed in the outer membrane of Gram-negative bacteria. They should be detectable in the sequence because every second residue is nonpolar. A closer inspection, however, shows that the significance of this information is low, because the individual β-strands are only slightly more than half a dozen residues long and the intermittent residues pointing to the barrel interior can be both polar and nonpolar.

At present, transmembrane β-barrel proteins have been found exclusively in the outer membrane of Gram-negative prokaryotes, and these membranes seem to lack α-helical proteins. Accordingly, a separation exists between α-proteins in all cytoplasmic membranes and β-proteins in the specialized outer membranes. Following the endosymbiotic

* Tel.: +49-761-203-6058; fax: +49-761-203-6161.
E-mail address: schulz@bio.chemie.uni-freiburg.de (G.E. Schulz).

0005-2736/02/$ - see front matter
PII: S0005-2736(02)00577-1

hypothesis, β-proteins are also expected in the outer membranes of mitochondria and chloroplasts, but none of these proteins has yet been structurally established. Given the limited abundance of such membranes, the β-proteins are likely to make up only a small, special class of membrane proteins.

The presently known structures indicate that the number of distinct chain folds of integral membrane proteins is probably much smaller than the respective number of water-soluble proteins, which ranges around a thousand [3,4]. The proteins of the cytoplasmic membrane consist mostly of transmembrane α-helices, and the bacterial outer membrane proteins contain β-barrels. Both types show a high neighborhood correlation which limits the number of different topologies appreciably [5]. The α-helices run, in general, perpendicular to the membrane plane and connections are formed between neighboring helix ends [6]. Moreover, all transmembrane β-barrels contain meandering all-next-neighbor antiparallel sheets, the topologies of which are simple and completely described by the number of strands.

2. Observed membrane protein structures

X-ray diffraction analysis is a suitable and convenient method for obtaining exact structures of membrane proteins, but it requires three-dimensional crystals. Membrane protein crystallization has always been a bottleneck. Part of this obstacle is the preparation of sufficient homogeneous membrane protein material, because the limited volume of the two-dimensional entity membrane cannot incorporate large amounts of a recombinant protein. Moreover, any tampering with the membrane is highly hazardous to the respective organism so that high expression levels are generally rare. This problem was circumvented by expressing a membrane protein into the cytosol and (re)naturing it therefrom into micelles [7], which is possible for a number of β-barrel proteins.

As a general observation, the crystallization of the bacterial outer membrane proteins appears to be easier than that of the α-helical proteins from the plasma membrane. Accordingly, the list of structurally established β-barrel membrane proteins is comparatively long (Table 1). The resolution of the analyses ranges from 1.6 Å for OmpA (neglecting the non-native gramicidin-A crystals) to 3.2 Å for the porin OmpC (OmpK36). The crystals are usually loosely packed, except for one crystal form of OmpA that reached 50% (v/v) protein in the crystal but diffracted merely to medium resolution [8].

The very existence of β-barrels was established for chymotrypsin at a very early stage in the now common protein crystal structure analysis. This enzyme contains two distorted six-stranded β-barrels with identical topologies [9]. Further β-barrels in water-soluble proteins are TIM-barrels [10] and those of streptavidin [11] and of the lipocalins [12]. The β-helices belong also to this group as they can be taken as single-stranded β-barrels ($n=1$) with large shear numbers of $S=18$ and more (see below). They were first detected with pectate lyase [13]. The right-handed and left-handed versions have positive and negative S-values, respectively. The cross sections of these β-helical barrels deviate drastically from circles, resembling boomerangs, flat ellipses [14] and triangles [15].

The pentadecameric antibiotic peptide, gramicidin A, forms channels through membranes that allow the passage of alkali ions. It has been included in Table 1 because it forms a β-helix, the structure of which was determined by

Table 1
Membrane proteins consisting of β-barrels[a]

	n	S	R (Å)[b]	α (deg)[b]	Oligomeric state
Gramicidin A (native)	1	6	3.4	77	Head-to-head dimer traversing the membrane
Nanotube	1	–	5.6	90	Stack of about eight cyclic octapeptides through the membrane
OmpX	8	8	7.2	37	Monomer without channel
OmpA	8	10	7.9	43	Monomer without channel
OmpT	10	12	9.5	42	Monomer without channel
OmpLA[c]	12	12	10.6	37	Monomer without channel
TolC	12	20	13.6	51	Single β-barrel composed of a trimer, forms a channel
α-Haemolysin	14	14	12.3	37	Single β-barrel composed of a heptamer, forms a channel
Porin *Rhodobacter capsulatus*	16	20	15.5	43	Trimer of parallel β-barrels forming three channels
Porin OmpF (PhoE, OmpC)	16	20	15.5	43	Trimer of parallel β-barrels forming three channels
Porin *Rhodobacter blasticus*	16	20	15.5	43	Trimer of parallel β-barrels forming three channels
Porin *Paracoccus denitrificans*	16	20	15.5	43	Trimer of parallel β-barrels forming three channels
Porin Omp32	16	20	15.5	43	Trimer of parallel β-barrels forming three channels
Maltoporin (two species)	18	20	17.1	40	Trimer of parallel β-barrels forming three channels
Sucrose porin	18	20	17.1	40	Trimer of parallel β-barrels forming three channels
FhuA	22	24	19.9	39	Monomer clogged by a removable polypeptide domain
FepA	22	24	19.9	39	Monomer clogged by a removable polypeptide domain

[a] All sheets are antiparallel except for native gramicidin A. The topologies are always all-next-neighbor.
[b] The radius is calculated for a circular cross section. The angle α can vary by ± 15° around the barrel (Fig. 1).
[c] This enzyme exists as a monomer in the membrane and becomes active on dimerization.

solid-state NMR [16]. Two of these β-helices associate head-to-head forming a channel through the membrane. Such narrow barrels can only be assumed if L-amino acid residues alternate with D-amino acids (or glycines) along the peptide chain, and here this is actually the case. The artificial nanotubes listed in Table 1 follow the design of the gramicidin A channel except that the chain is an eight-membered ring instead of a β-helix [17]. The rings are stacked, forming a channel.

The bacterial outer membrane protein OmpX consists of the smallest established transmembrane β-barrel of the canonical type [18]. Its barrel contains $n=8$ strands with a shear number $S=8$ and appears to represent the minimum construction for a transmembrane β-protein (Table 1). In contrast to OmpX, the ubiquitous outer membrane protein A possesses an N-terminal 171-residue domain (here called OmpA) as a membrane anchor and a C-terminal periplasmic domain binding to the peptidoglycan cell wall. OmpA contains an eight-stranded β-barrel with a shear number $S=10$, which is larger than that of OmpX, giving rise to a larger barrel cross section [19]. Applying point mutations, the OmpA crystals were improved to diffract to 1.6 Å resolution [8]. This allowed for an anisotropic structure refinement revealing the major mobility directions of loops and turns. It demonstrated that the loops and turns have asymmetric mobilities that correspond to those of a model in which the polypeptide is represented by a resilient wire.

Somewhat larger β-barrels were observed with enzymes found in the bacterial outer membranes. One of these enyzmes is the protease OmpT consisting of a 10-stranded β-barrel with a shear number $S=12$ [20]. While the 'lower' part of the β-barrel is immersed in the membrane as usual, its 'upper' part protrudes to the external medium and contains the catalytic center where foreign proteins are split. OmpT is of medical interest because it contributes to the pathogenicity of bacteria. A further surfacial enzyme is the phospholipase A (OmpLA) that destroys lipopolysaccharides. It consists of a 12-stranded β-barrel with a shear number $S=12$ [21]. Its barrel contains a solid interior hydrogen bonding network without a pore, a nonpolar outer surface, and the catalytic center at the external end. OmpLA is active as a dimer accommodated in the membrane.

A special variety of β-barrels was found in TolC [22] and in α-haemolysin [23]. These barrels are composed of several portions coming from different subunits (Table 1). The TolC barrel consists of three four-stranded all-next-neighbor antiparallel β-sheet pieces coming from the three subunits. The major parts of the subunits are α-helical and not in the outer membrane. The shear number S is as large as 20, giving rise to a wide channel along the barrel axis. This is in contrast to the 12-stranded β-barrel of OmpLA which has a smaller S and a solid core. The α-haemolysin barrel consists of seven β-hairpin loops coming from the seven subunits. Each subunit is water-soluble. The β-hairpin loop undergoes a large conformational change during the cooperative process of β-barrel formation, which is likely to occur on membrane insertion and after the large globular parts have formed an annular heptamer [24].

Abundant proteins of the bacterial outer membrane are porins which form passive channels showing various grades of selectivity. The most common type consists of 16-stranded β-barrels with a shear number $S=20$. A typical structure is that of the porin from *R. blasticus* illustrated in Fig. 1. After the structure of a photoreaction center was established [25], the second membrane protein structure known at atomic resolution was that of a porin [26,27]. It revealed numerous general construction principles [28,29], which were subsequently also observed in other membrane proteins (e.g. the aromatic girdles), in other transmembrane β-barrels (e.g. the short periplasmic turns), and in the other porins of this type (e.g. the transversal electric field for polarity separation). The structures of two channels that are highly selective for maltooligosaccharides and sucrose, respectively, showed 18-stranded barrels with kidney-shaped cross sections [30–32]. These cross sections deviate strongly from circles and allow long narrow channels which are required for the selection process.

As listed in Table 1, the largest β-barrels have been observed with the monomeric iron transporter proteins FhuA and FepA. The structure of FhuA was established independently by two groups [33,34]. It is known with and without a ligated siderophore. The structure of the ferric enterobactin receptor FepA is homologous to FhuA showing identical topology and a similar transport mechanism [35]. In both cases, there are more than 700 residues assembled in two domains: an N-terminal 150-residue domain is located inside a C-terminal 22-stranded β-barrel with a shear number $S=24$.

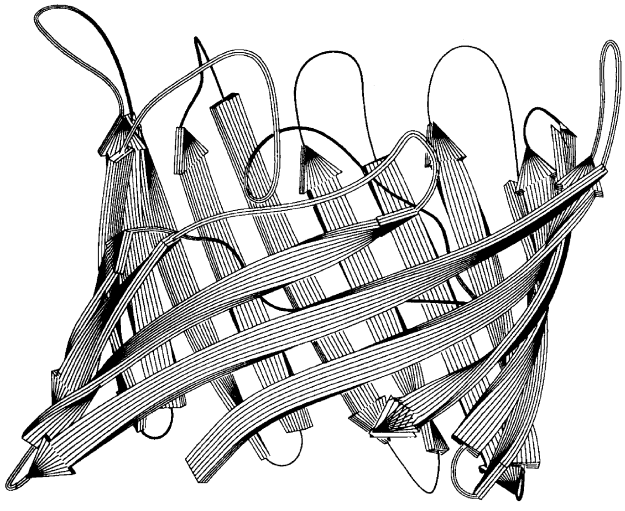

Fig. 1. Ribbon plot of the 16-stranded β-barrel of the general porin from *R. blasticus* viewed from the molecular threefold axis [72]. Note the large variation of the inclination angle α and the difference between the high barrel wall facing the membrane in the rear and the low wall at the trimer interface in the front.

3. β-Barrel design

The construction principles of β-barrels are illustrated in Fig. 2. Here, the cylindrical barrel has been cut where the first strand reaches the upper barrel end and then flattened out. The view is from outside the barrel. All β-strands are assumed to run in the same inclination angle α. The β-pleated sheet parameters $a = 3.3$ Å and $b = 4.4$ Å refer to all kinds of β-sheets: parallel, antiparallel or mixed. The hydrogen bonds are sketched for the predominant antiparallel sheet. The relationship between the number of strands n, the shear number S and the tilt angle α becomes obvious:

$$R = [(Sa)^2 + (nb)^2]^{0.5}/2\pi$$

$$\tan\alpha = Sa/nb$$

$$R = nb/2\pi\cos\alpha \quad \text{(circular cross section)}$$

The shear number S comes with a sign. Negative values are observed in the special cases of β-helices (left-handed). In canonical β-barrels, S is positive and ranges between n and $n+4$ allowing for an optimum β-sheet twist (Table 1). TolC with $S = n+8$ is an exception. Furthermore, S is always an even number because after running around the barrel, ridges and valleys of the pleated sheet have to be joined to ridges and valleys again. In other words, the hydrogen bonds repeat only every second residue.

A graphic display of the relationship between n, S and α of β-barrels is given in Fig. 3. The smallest barrel of the canonical type has six strands, two strongly distorted copies

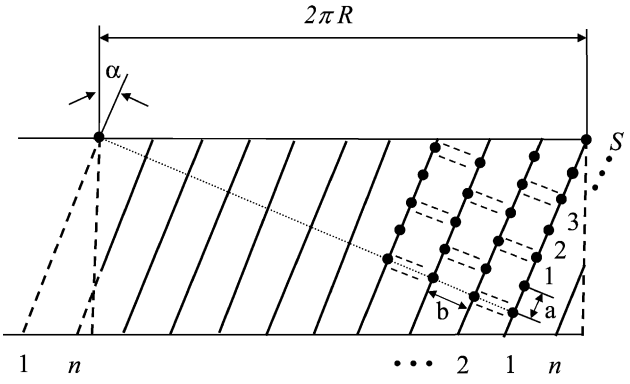

Fig. 2. General architecture of a β-barrel which here is assumed to be circular. The description depends neither on the sequence of the strands nor on their directions. Residues are represented by their Cα atoms. The barrel is cut where the first strand reaches the upper end, flattened out and viewed from the outside. The depicted barrel contains $n = 10$ β-strands. The dotted line follows a pleat of the sheet, that is, the hydrogen bonds. The shear number S is derived by running from a given strand (here no. 1) to the left along the hydrogen bonds once around the barrel and counting the residue number S to the point of return to the same strand [73–75]. The displayed β-barrel has a shear number S of +6. The depicted β-strand tilt corresponds to a positive S value, and a tilt to the left to a negative S. The inclination angle α is about 20°.

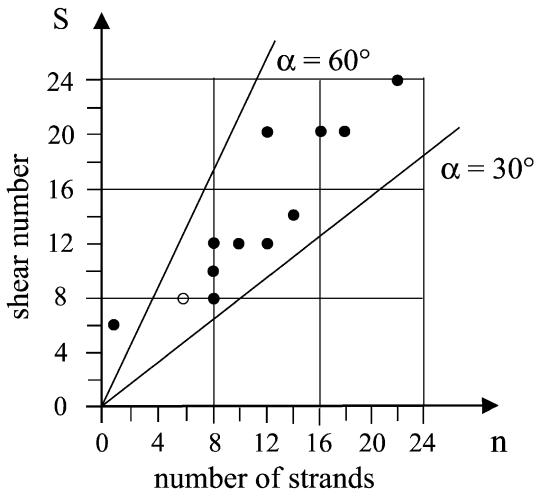

Fig. 3. The observed β-barrels concentrate at tilt angles α between 30° and 60°. Because of the two-residue-repeat in the hydrogen bond pattern (Fig. 2), the shear number S is always even in completely antiparallel barrels. The radius R of the barrel increases with the number of strands n as well as with the shear number S. Up to OmpLA ($n = S = 12$), the interior of the barrel can be filled by side chains and fixed water molecules. The open circle corresponds to the two distorted six-stranded β-barrels in the water-soluble enzyme chymotrypsin, which were the first barrels to be detected [9].

of it were found in chymotrypsin. Eight-stranded β-barrels are more regular and much more common. Among the water-soluble proteins, there is a series of eight-stranded barrels with shear numbers ranging from 8 in TIM, over 10 in streptavidin, to 12 in the lipocalins. In all these cases, the barrel interior contains a hydrophobic core. In the abundant TIM-barrels, the active centers are invariably found at the carboxyterminal end of the barrel. Streptavidin binds biotin at one barrel end. The same applies for lipocalins where the bound large nonpolar compounds reach down to the barrel center. The increasing ligand sizes and binding site depths from TIM over streptavidin to the lipocalins correspond to the increasing barrel radii caused by larger shear numbers.

Whereas the water-soluble proteins have β-barrels up to 8 strands, those of membrane-inserted β-barrels start at 8 strands and run up to 22 (Table 1). Presumably, the required tightly packed nonpolar barrel core of water-soluble proteins limits the radius of circular barrels to small values. In contrast, transmembrane barrels form polar cores, the stability of which depends on hydrogen bonds rather than on geometrically exact nonpolar packing contacts. Such polar cores can be constructed much more easily and may also include water molecules that increase the interior volume. Accordingly, the interiors of the barrels with up to 12 strands are polar and solid, except for TolC with its exceptionally large shear number of 20. The large shear number gives rise to a large barrel radius which causes TolC to form a channel. The same applies for α-haemolysin which, however, has a smaller shear number but two more β-strands.

Channels are of course also formed by all porins. A general porin contains 16 β-strands, has a shear number of

20 and a nearly circular cross section (Table 1, Fig. 1). Three parallel barrels associate to form trimers. The type of residues outlining the channel determines the specificity of such a general porin which, however, is usually not very strict. The two 18-stranded porins are very specific. Their channel cross sections are actually smaller than those of the general porins in agreement with their higher selectivity. The 22-stranded barrels of the iron transporter proteins have circular cross sections and would form a very wide channel if they were not filled with the globular N-terminal 150-residue domain.

In addition to the construction principles dictated by the β-barrel geometry and illustrated in Fig. 2, the transmembrane β-barrels follow further rules that are probably dictated by factors other than the covalent peptide structure:

I. All β-strands are antiparallel and locally connected to their next neighbors.
II. Both the N- and C-termini are at the periplasmic barrel end restricting the strand number *n* to even values.
III. On trimerization, a nonpolar core is formed at the molecular threefold axis of the porins so that the central part of the trimer resembles a water-soluble protein.
IV. The external β-strand connections are long loops named L1, L2, etc., whereas the periplasmic strand connections are generally minimum-length turns named T1, T2, etc.
V. Cutting the barrel as shown in Fig. 2 and placing the periplasmic end at the bottom, the chain runs from the right to the left.
VI. In all porins, the constriction at the barrel center is formed by an inserted long loop L3.
VII. The β-barrel surface contacting the nonpolar membrane interior is coated with aliphatic side chains forming a nonpolar ribbon. The two rims of this ribbon are lined by girdles of aromatic side chains.
VIII. The sequence variability in transmembrane β-barrels is higher than in water-soluble proteins and exceptionally high in the external loops.

Rules I, II and III are likely to reflect the folding process of the trimeric porins. Presumably, the central part folds in the periplasm like a water-soluble protein. The membrane-exposed parts of the barrels are then formed on insertion into the membrane. The short turns of rule IV may facilitate barrel formation inside the membrane. Presumably, rule V is a consequence of rule IV because appropriate short turns can only be formed in one of the two possible chain directions. Rule VI seems to reflect an early evolutionary event that has not yet been revised. The aromatic girdles of rule VII are illustrated in detail in Fig. 4. The aromatic side chains were suggested as stabilizers of the β-barrel and of its vertical position in the membrane [28]. The stabilization has been confirmed experimentally by demonstrating the preference of aromatic compounds for the two nonpolar–polar transition regions of the membrane [36,37]. Rule VIII came as a surprise to those with a high respect for membrane proteins which, of course, is mainly caused by our difficulties in solving membrane protein structures. Rule VIII explains these difficulties because it indicates that membrane proteins are subjected to fewer structural restraints than water-soluble ones and for this reason are, in general, more mobile and thus less crystallizable.

In view of the drastic mobility differences between the external loops and the membraneous and periplasmic moieties of the barrels, it was suggested that these proteins can be crystallized by creating suitable packing contacts through

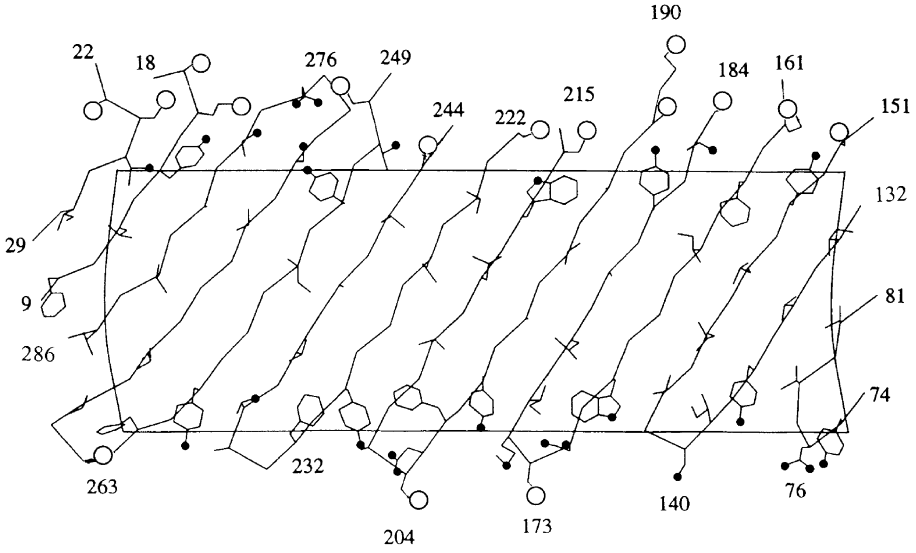

Fig. 4. The β-barrel of *R. blasticus* [72], which is depicted in Fig. 1, cut near the molecular threefold axis and viewed from the outside as in Fig. 2. The membrane-facing part is outlined. It consists of a ribbon of aliphatic nonpolar residues with two girdles of aromatic residues. Note that the polar atoms (black dots) of the aromatic side chains point to the polar layers of the membrane. The aromatic side chains can rotate quickly around their Cα–Cβ bond which is perpendicular to the β-sheet plane.

semi-random mutagenesis at loops and turns [38]. Without structural knowledge, these loops and turns can often be predicted from the sequence and from interaction studies. For OmpA and OmpX, this approach resulted in surprising successes. The procedure is also applicable to α-helical membrane proteins in as much as their crystallization problem is governed by their small polar surfaces. It is quite possible, however, that they hestitate to crystallize because their transmembrane α-helices are stabilized by the native laminar membrane environment and become flexible in the detergent/lipid micelles used for crystallization.

Given so many rules, the prediction of transmembrane β-barrels from the sequence should be achievable at a high confidence level. However, the simple approach of looking for alternating polar and nonpolar residues inside and outside the barrel is not very helpful because this pattern is frequently broken by nonpolar residues on the inside. Moreover, the β-strands are merely slightly more than half a dozen residues long which limits their information content appreciably. These problems have been tackled in several prediction programs [39–44] but cannot be considered solved. For some time to come, the safety of β-barrel prediction will remain well below that of transmembrane α-helices with their simple nonpolar 25-residue segments.

4. Functions of outer membrane proteins

After discussing the structures, it seems appropriate to refer also to the functions. OmpX is synthesized in large amounts in stress situations and it is probably used as a defensive weapon binding to and thus interfering with foreign proteins. Half of the OmpX β-barrel protrudes into the external medium, presenting an inclined β-sheet edge that binds to any foreign protein with a β-strand in its surface layer [18]. Such proteins are ubiquitous, an example being the large group of proteins with central parallel β-sheets surrounded by α-helices. In the X-ray analysis, all loop residues of OmpX were located in electron density indicating that the β-sheet edge presented to the foreign proteins is rigid, as it is required for tight binding. In contrast to OmpX, the long external loops of OmpA are highly mobile and for the most part not visible in the respective electron density map. In vivo, the mobile loops are rather resistant to proteolytic attack, presumably because they bind to the surrounding lipopolysaccharides. Obviously, the mobile loops fulfill essential functions in bacterial life [45].

The outer membrane enzyme OmpT is a special protease that has been implicated in the pathogenicity of bacteria. It is monomeric with the active center pointing to the outside [20]. A further enzyme, the phospholipase A OmpLA, produces holes in the outer membrane when it is activated. The activation process has not yet been clarified, but it is known to require a dimerization of OmpLA in the membrane. The activation by dimer formation has been verified by a crystal structure analysis of an OmpLA dimer which was produced by a reaction with an inhibitor [21]. It showed that the essential active center residues are distributed over both subunits. The active centers are well placed for deacylating lipopolysaccharides of the external leaflet of the outer bacterial membrane. OmpLA functions in the secretion of colicins and virulence factors.

The general porins with 16-stranded β-barrels (Table 1) contain pores with sizes allowing the permeation of molecules up to molecular masses of about 600 Da [46]. The pores come with various selectivities. The porin from *R. capsulatus*, for instance, contains a rather nonpolar binding site near the external end of the pore eyelet, indicating that it may pick up molecules such as adenosine at very low concentrations. The structure also revealed a transversal electric field across the pore eyelet that acts as a polarity separator, excluding the unwanted nonpolar compounds [28]. Porin OmpF from *Escherichia coli* has been thoroughly analyzed by numerous groups and became the first membrane protein to form X-ray grade crystals [47]. It is closely homologous to the porins PhoE [48] and OmpC. These three porins show permeation properties adjusted to different environmental conditions. PhoE allows an efficient uptake of phosphate. OmpC from *E. coli* and its homologue OmpK36 from *Klebsiella pneumoniae* [49] are osmoporins that are expressed at high osmotic pressures usually caused by high salt concentrations. The high-salt OmpC differs from the low-salt OmpF mainly by an increased number of charged residues pointing into the pore lumen. Presumably, the charge increase counteracts Debye–Hückel shielding at high ionic strength so that OmpF and OmpC (OmpK36) have comparable permeation properties in differing environments.

Further structures were established for the main porin from *Paracoccus denitrificans* [50] and for Omp32 from *Comomonas acidovorans* [51]. They confirmed the established general features of their homologues. All structurally established porins are aggregates of three parallel β-barrels, each of which contains a single polypeptide chain. The β-barrels contain either 16 or 18 strands. The interfaces are usually large and tightly packed. Therefore, it is not conceivable that the subunits are stable as monomers, neither in the membrane nor in the periplasm. However, the existence of a functional monomeric porin has been reported [52], but its structure is not yet elucidated.

The highly specific maltoporin has a small pore that is adapted to the amylose helix and accepts only glucose units [30,31]. The energetics of a maltooligosaccharide diffusing through such a pore has been examined in detail, revealing a combination of nonpolar and optimally spaced polar interactions that results in smooth gliding [53]. This energy profile has been confirmed in a molecular dynamics study [54] and in an experimental study based on mutants [55]. The sucrose porin is a homologue of the maltoporin and very specific for the small molecule sucrose, which is much smaller than the oligomers accepted by maltoporin [32].

Besides porin trimers with 16- and 18-stranded β-barrels, even larger 22-stranded β-barrel proteins were found in the outer membrane, namely the monomeric active iron transporters FhuA and FepA. The lack of ATP or an equivalent energy carrier in the periplasm restricts the outer membrane in the first place to more or less specific but passive pores that are not able to transport any solute against a concentration gradient. The bacteria overcame this problem by inventing plugged β-barrels and the TonB apparatus. The structures of the two evolutionarily related plugged pores FhuA and FepA are known. Their β-barrels have diameters of about 40 Å (Table 1). They bind siderophore-encapsulated iron in the external half of the barrel and are obstructed by an N-terminal 150-residue domain in the periplasmic barrel half. Mutational studies have revealed their TonB binding sites. The directed iron transport through the outer membrane is energized by an interaction with TonB of the inner membrane that can draw energy from the cytosolic ATP pool [56,57]. The plug formed by the 150-residue domain is removed after binding to TonB, making the siderophore available for internalization.

The heptameric α-haemolysines A follow a completely different principle [23,24]. These proteins associate with their extra-membrane domains. Subsequently, each subunit donates a β-hairpin to form a common 14-stranded β-barrel through the membrane. In a similar manner, TolC is assembled from three α-helical subunits [22]. The subunits form a long, wide channel that spans the periplasm in their α-helical part and that is prolonged through the outer membrane by the β-barrel. The channel is used for the export of xenobiotics.

The endosymbiotic theory suggests that the outer membrane of Gram-negative bacteria corresponds to the outer membranes of mitochondria and chloroplasts [58]. All of them are porous and cannot hold an electric potential difference. One long-term candidate for a porin homologue is the voltage-dependent anion channel (VDAC) of the outer mitochondrial membrane [59]. A further candidate for a β-barrel channel in the outer mitochondrial membrane is Tom40, which contains β-structure and forms a pore [60]. Its molecular mass would suggest a β-barrel of the size of general porins. Unfortunately, none of these proteins has yielded crystals suitable for structure analysis yet. Presumably, they are particularly difficult to crystallize because they face the soft cytosol, which does not require tough structures, in contrast to their bacterial counterparts that face the external medium demanding much higher stability.

5. Folding, stability and engineering

In general, the folding process of β-proteins should be much more complex than that of α-proteins. This does not apply, however, for the all-next-neighbor antiparallel transmembrane β-barrels discussed here. For the porins, it was suggested that the central part of the homotrimer including all N- and C-termini folds in the periplasm like a water-soluble protein so that the membrane-facing parts of the β-barrels dangle as 200-residue loops into the solvent [28]. On membrane insertion, these loops can then easily meander forming the special β-sheet topology. The simplicity of the folding process is corroborated by the fact that porins and other transmembrane β-barrels such as OmpA [19] can be (re)natured from inclusion bodies. This production method worked even for the large monomeric β-barrel of FepA [35].

Engineering experiments with OmpA demonstrated that the β-barrel itself is rather stable. The four external loops of OmpA were replaced by short-cuts in all possible combinations [61]. The resulting deletion mutants lost their biological functions in bacterial *F*-conjugation and as bacteriophage receptors, but kept the transmembrane β-barrel as demonstrated by their resistance to proteolysis and thermal denaturation. The experiments confirm the expectation that the large external loops do not contribute to β-barrel folding and stability.

In α-haemolysin, the β-strand sequence was altered by reversing the sequence within the β-hairpin contributed by each subunit to the β-barrel [62]. With respect to the β-barrel, this changed only the hydrogen bonding pattern, but it reversed the sequence in the β-turn at the hairpin end and should therefore have local conformational consequences. It turned out that the ‘retro’-barrel formed a channel but failed to function properly as it could not invade erythrocytes. A high activity could be obtained, however, when the β-turn was left in its original amino acid sequence, demonstrating that the tight β-turns at one end of these barrels are important for the stability of the whole barrel. Unfortunately, the detailed structures of the ‘retro’-barrels remain unknown.

The interiors of the four small β-barrels of OmpA, OmpX, OmpT and OmpLA are filled with polar residues forming a hydrogen bonding network. A number of separated cavities mostly filled with water have been reported for OmpA and OmpX. Accordingly, these β-proteins are rigid inverse micelles and not likely to form pores. For OmpA, there was a lengthy discussion on the question of pore formation because small pores had actually been detected by ion fluxes [63,64]. Presumably, these data were obtained with OmpA preparations that had lost the internal barrel structure during the protein purification process permitting channel formation. Such conformations should differ appreciably from the crystalline structure.

A functional feature attracting continuous interest is voltage-gating in porins. This effect remains to be explained in detail. It is observed at comparatively high voltages across the membrane. Since the corresponding electric field strength is so high that it may disrupt hydrogen bonds, it seems likely that most of the in vitro voltage-gating studies [65,66] report nothing other than a structural breakdown inside a pore. This does not apply to the voltage-dependent anion channel of the outer mitochondrial membrane (VDAC), however, which shows channel closure in vivo

[67]. Presumably, VDAC contains a solid but separate mobile and charged domain that can be driven by the electric field onto the pore so that it prevents any further ion flow.

Porins are passive diffusion channels. The diameters of their pore eyelets range from 10 Å for the general porins to 6 Å for the highly selective porins. Larger pores are usually decorated with oppositely charged residues at opposite sides that form a local transversal electric field at the pore eyelet. This field constitutes an energy barrier for low-polarity solutes [28] so that the bacterium can exclude unwanted nonpolar molecules such as antibiotics while presenting a spacious eyelet for collecting large polar molecules such as sugars.

The engineering of porins became popular after it had been demonstrated that a mass-produced porin (re)natured from inclusion bodies had assumed exactly the native conformation [7]. A systematic study changing the pore properties by mutations showed a strong correlation between eyelet cross section and diffusion rate [68]. Furthermore, a series of nine porins with mutations at the eyelet was analyzed with respect to ion conductance, ion selectivity and voltage-gating [66]. It was shown that charge reversals affect selectivity and voltage-gating. Similar results were obtained with mutation at loop L3 of PhoE [69]. In contrast to modifications at loop L3 inside the β-barrel, mutations at barrel wall residues lining the eyelet had only minor effects on voltage-gating. This corroborates the suggestion that voltage-gating reflects a structural breakdown in the pore. Sucrose porin has a somewhat larger pore than its homologue maltoporin, the pore eyelet of which is closely adjusted to $\alpha(1\rightarrow 4)$-bound glucose units [53]. With mutations at loop L3, the specificity of the sucrose porin was changed toward that of a maltoporin [70]. The specificity change was achieved by introducing three eyelet-defining residues of the maltoporin and by removing the additional N-terminal 70-residue domain of the sucrose porin, the structure of which is not yet known.

The ionic current through a black-lipid membrane harboring a membrane protein is a measure for the width of the respective passive channel. If the channel is clogged by organic molecules diminishing the current over the residence time of such a molecule, the reduction of the current as well as the time of residence are characteristic for the applied compound. Gu et al. [71] used this principle by placing a cyclodextrin as an adapter into the 14-stranded β-barrel of an engineered α-haemolysin and measuring the current reductions and the times of residence for a number of modified adamantans. They demonstrated that these molecules can be detected in concentrations around 10 μM and also identified by comparison with reference compounds.

Apart from the manifold possibilites of engineering on native β-barrels, these can also be designed ab initio. Ghadiri et al. [17] designed cyclic octapeptides and showed that these assemble to so-called ‘nanotubes’ forming channels through a membrane. The octapeptides consisted of alternating D- and L-amino acid residues and thus followed closely the construction principle of gramicidin A. In its native conformation, gramicidin A forms a single-stranded β-barrel ($n=1$) with a shear number $S=6$ that may also be called a β-helix (Table 1). The nanotubes are close to this construction, but form a ring with an inclination angle $\alpha=90^\circ$ instead of the helix. Stacking these rings through the membrane forms a β-barrel with a central channel.

6. Conclusions

Despite the predominance of α-helical transmembrane proteins, their β-barrel counterparts have become popular because many of them could be analyzed in atomic detail and at high resolutions. The transmembrane β-barrel proteins assume astonishingly regular conformations giving rise to numerous rules for their construction. These rules are likely to permit the detection of transmembrane β-barrels from the sequence at a reasonable confidence level in the future. It has been suggested that these regularities are required by the folding process.

While water-soluble proteins contain regular β-barrels with up to eight strands and nonpolar interiors, transmembrane β-barrels contain eight or more strands and have polar interiors. The smaller transmembrane β-barrels have solid cores partially filled with water. Accordingly, they can be considered inverse micelles. The larger barrels of this type have channels along their axis that allow the permeation of various types of solutes. The largest known 22-stranded transmembrane β-barrels are used for the active transport of rare commodities through the bacterial outer membrane. Their interior contains a globular protein domain which functions as a plug and can be removed for transport.

The success rate of engineering transmembrane β-barrels appears to be superior to that for soluble proteins. On one hand, these barrels can be mass produced into inclusion bodies and (re)natured therefrom in vitro. On the other hand, the interiors of the β-barrels housing the permeation channels can be mutated without affecting the barrel construction very much. This is in contrast to the situation with water-soluble protein where mutations are frequently punished by deterioration.

References

[1] J. Liu, B. Rost, Comparing function and structure between entire proteomes, Protein Sci. 10 (2001) 1970–1979.
[2] L. Sipos, G. von Heijne, Predicting the topology of eukaryotic membrane proteins, Eur. J. Biochem. 213 (1993) 1333–1340.
[3] G.E. Schulz, Protein differentiation: emergence of novel proteins during evolution, Angew. Chem., Int. Ed. Engl. 20 (1981) 143–151.
[4] S.E. Brenner, M. Levitt, Expectations from structural genomics, Protein Sci. 9 (2000) 197–200.
[5] G.E. Schulz, R.H. Schirmer, Principles of Protein Structure, Springer, New York, 1979, pp. 84–87.

[6] J.U. Bowie, Helix-bundle membrane protein fold templates, Protein Sci. 8 (1999) 2711–2719.
[7] B. Schmid, M. Krömer, G.E. Schulz, Expression of porin from *Rhodopseudomonas blastica* in *Escherichia coli* inclusion bodies and folding into exact native structure, FEBS Lett. 381 (1996) 111–114.
[8] A. Pautsch, G.E. Schulz, High resolution structure of the OmpA membrane domain, J. Mol. Biol. 298 (2000) 273–282.
[9] J.J. Birktoft, D.M. Blow, Structure of crystalline α-chymotrypsin, J. Mol. Biol. 68 (1972) 187–240.
[10] D.W. Banner, A.C. Bloomer, G.A. Petsko, D.C. Phillips, C.I. Pogson, I.A. Wilson, P.H. Corran, A.J. Furth, J.D. Milman, R.E. Offord, J.D. Priddle, S.G. Waley, Structure of chicken muscle triose phosphate isomerase determined crystallographically at 2.5 Å resolution using amino acid sequence data, Nature 255 (1975) 609–614.
[11] W.A. Hendrickson, A. Pähler, J.L. Smith, Y. Satow, E.A. Merritt, R.P. Phizackerley, Crystal structure of core streptavidin determined from multi-wavelength anomalous diffraction of synchrotron radiation, Proc. Natl. Acad. Sci. U. S. A. 86 (1989) 2190–2194.
[12] M.E. Newcomer, T.A. Jones, J. Åqvist, J. Sundelin, U. Eriksson, L. Rask, P.A. Peterson, The three-dimensional structure of retinol-binding protein, EMBO J. 3 (1984) 1451–1454.
[13] M.D. Yoder, N.T. Keen, F. Jurnak, New domain motif: the structure of pectate lyase C, a secreted plant virulence factor, Science 260 (1993) 1503–1507.
[14] U. Baumann, S. Wu, K.M. Flaherty, D.B. McKay, Three-dimensional structure of the alkaline protease of *Pseudomonas aeruginosa*: a two-domain protein with a calcium binding parallel beta roll motif, EMBO J. 12 (1993) 3357–3364.
[15] C.R.H. Raetz, S.L. Roderick, A left-handed parallel β-helix in the structure of UDP-*N*-acetylglucosamine acyltransferase, Science 270 (1995) 997–1000.
[16] R.R. Ketchem, W. Hu, T.A. Cross, High-resolution conformation of gramicidin A in a lipid bilayer by solid-state NMR, Science 261 (1993) 1457–1460.
[17] M.R. Ghadiri, J.R. Granja, L.K. Buehler, Artificial transmembrane ion channels from self-assembling peptide nanotubes, Nature 369 (1994) 301–304.
[18] J. Vogt, G.E. Schulz, The structure of the outer membrane protein OmpX from *Escherichia coli* reveals possible mechanisms of virulence, Structure 7 (1999) 1301–1309.
[19] A. Pautsch, G.E. Schulz, Structure of the outer membrane protein A transmembrane domain, Nat. Struct. Biol. 5 (1998) 1013–1017.
[20] L. Vandeputte-Rutten, R.A. Kramer, J. Kroon, N. Dekker, M.R. Egmond, P. Gros, Crystal structure of the outer membrane protease OmpT from *Escherichia coli* suggests a novel catalytic site, EMBO J. 20 (2001) 5033–5039.
[21] H.J. Snijder, I. Ubarretxena-Belandia, M. Blaauw, K.H. Kalk, H.M. Verhij, M.R. Egmond, N. Dekker, B.W. Dijkstra, Structural evidence for dimerization-regulated activation of an integral membrane phospholipase, Nature 401 (1999) 717–721.
[22] V. Koronakis, A. Scharff, E. Koronakis, B. Luisi, C. Hughes, Crystal structure of the bacterial membrane protein TolC central to multidrug efflux and protein export, Nature 405 (2000) 914–919.
[23] L. Song, M.R. Hobaugh, C. Shustak, S. Cheley, H. Bayley, J.E. Gouaux, Structure of staphylococcal α-hemolysin, a heptameric transmembrane pore, Science 274 (1996) 1859–1865.
[24] R. Olson, H. Nariya, K. Yokota, Y. Kamio, E. Gouaux, Crystal structure of Staphylococcal LukF delineates conformational changes accompanying formation of a transmembrane channel, Nat. Struct. Biol. 6 (1999) 134–140.
[25] J. Deisenhofer, O. Epp, K. Miki, R. Huber, H. Michel, Structure of the protein subunits in the photosynthetic reaction centre of *Rhodopseudomonas viridis* at 3 Å resolution, Nature 318 (1985) 618–624.
[26] M.S. Weiss, T. Wacker, J. Weckesser, W. Welte, G.E. Schulz, The three-dimensional structure of porin from *Rhodobacter capsulatus* at 3 Å resolution, FEBS Lett. 267 (1990) 268–272.
[27] M.S. Weiss, G.E. Schulz, Structure of porin refined at 1.8 Å resolution, J. Mol. Biol. 227 (1992) 493–509.
[28] G.E. Schulz, Structure–function relationships in the membrane channel porin as based on a 1.8 Å resolution crystal structure, in: A. Pullman, J. Jortner, B. Pullman (Eds.), Membrane Proteins: Structures, Interactions and Models, Kluwer, Dordrecht, 1992, pp. 403–412.
[29] G.E. Schulz, Structure–function relationships in porins as derived from a 1.8 Å resolution crystal structure, in: J.M. Ghuysen, R. Hakenbeck (Eds.), New Comprehensive Biochemistry, Bacterial Cell Wall, vol. 27, Elsevier, Amsterdam, 1994, pp. 343–352.
[30] T. Schirmer, T.A. Keller, Y.F. Wang, J.P. Rosenbusch, Structural basis for sugar translocation through maltoporin channels at 3.1 Å resolution, Science 267 (1995) 512–514.
[31] J.E.W. Meyer, M. Hofnung, G.E. Schulz, Structure of maltoporin from *Salmonella typhimurium* ligated with a nitrophenyl-maltrotrioside, J. Mol. Biol. 266 (1997) 761–775.
[32] D. Forst, W. Welte, T. Wacker, K. Diederichs, Structure of the sucrose-specific porin ScrY from *Salmonella typhimurium* and its complex with sucrose, Nat. Struct. Biol. 5 (1998) 37–46.
[33] K.P. Locher, B. Rees, R. Koebnik, A. Mitschler, L. Moulinier, J.P Rosenbusch., D. Moras, Transmembrane signaling across the ligand-gated FhuA receptor: crystal structures of free and ferrichrome-bound states reveal allosteric changes, Cell 95 (1998) 771–778.
[34] A.D. Ferguson, E. Hofmann, J.W. Coulton, K. Diederichs, W. Welte, Siderophore-mediated iron transport: crystal structure of FhuA with bound lipopolysaccharide, Science 282 (1998) 2215–2220.
[35] S.K. Buchanan, B.S. Smith, L. Venkatramani, D. Xia, L. Esser, M. Palnitkar, R. Chakraborty, D. van der Helm, J. Deisenhofer, Crystal structure of the outer membrane active transporter FepA from *Escherichia coli*, Nat. Struct. Biol. 6 (1999) 56–63.
[36] W.C. Wimley, S.H. White, Experimentally determined hydrophobicity scale for proteins at membrane interfaces, Nat. Struct. Biol. 3 (1996) 842–848.
[37] W.M. Yau, W.C. Wimley, K. Gawrisch, S.H. White, The preference of tryptophan for membrane interfaces, Biochemistry 37 (1998) 14713–14718.
[38] A. Pautsch, J. Vogt, K. Model, C. Siebold, G.E. Schulz, Strategy for membrane protein crystallization exemplified with OmpA and OmpX, Proteins: Struct. Funct. Genet. 34 (1999) 167–172.
[39] W. Welte, M.S. Weiss, U. Nestel, J. Weckesser, E. Schiltz, G.E. Schulz, Prediction of the general structure of OmpF and PhoE from the sequence and structure of porin from *Rhodobacter capsulatus*. Orientation of porin in the membrane, Biochim. Biophys. Acta 1080 (1991) 271–274.
[40] T. Schirmer, S.W. Cowan, Prediction of membrane-spanning β-strands and its application to maltoporin, Protein Sci. 2 (1993) 1361–1363.
[41] M.M. Gromiha, R. Majumdar, P.K. Ponnuswamy, Identification of membrane spanning β-strands in bacterial porins, Protein Eng. 10 (1997) 497–500.
[42] K. Seshadri, R. Garemyr, E. Wallin, G. von Heijne, A. Elofsson, Architecture of β-barrel membrane proteins: analysis of trimeric porins, Protein Sci. 7 (1998) 2026–2032.
[43] K. Diederichs, J. Freigang, S. Umhau, K. Zeth, J. Breed, Prediction by a neural network of outer membrane β-strand protein topology, Protein Sci. 7 (1998) 2413–2420.
[44] I. Jacoboni, P.L. Martelli, P. Fariselli, V. de Pinto, R. Casadio, Prediction of the transmembrane regions of β-barrel membrane proteins with a neural network-based predictor, Protein Sci. 10 (2001) 779–787.
[45] R. Morona, M. Klose, U. Henning, *Escherichia coli* K-12 outer membrane protein (OmpA) as a bacteriophage receptor: analysis of mutant genes expressing altered proteins, J. Bacteriol. 159 (1984) 570–578.
[46] H. Nikaido, Prevention of drug access to bacterial targets: permeability barriers and active efflux, Science 264 (1994) 382–388.
[47] R.M. Garavito, J.P. Rosenbusch, Three-dimensional crystals of an integral membrane protein: an initial X-ray analysis, J. Cell Biol. 86 (1980) 327–329.

[48] S.W. Cowan, T. Schirmer, G. Rummel, M. Steiert, R. Ghosh, R.A. Pauptit, J.N. Jansonius, J.P. Rosenbusch, Crystal structures explain functional properties of two *E. coli* porins, Nature 358 (1992) 727–733.
[49] R. Dutzler, G. Rummel, S. Alberti, S. Hernández-Allés, P.S. Phale, J.P. Rosenbusch, V.J. Benedi, T. Schirmer, Crystal structure and functional characterization of OmpK36, the osmoporin of *Klebsiella pneumoniae*, Structure 7 (1999) 425–434.
[50] A. Hirsch, J. Breed, K. Saxena, O.M.H. Richter, B. Ludwig, K. Diederichs, W. Welte, The structure of porin from *Paracoccus denitrificans* at 3.1 Å resolution, FEBS Lett. 404 (1997) 208–210.
[51] K. Zeth, K. Diederichs, W. Welte, H. Engelhardt, Crystal structure of Omp32, the anion-selective porin from *Comamonas acidovorans*, in complex with a periplasmic peptide at 2.1 Å resolution, Structure 8 (2000) 981–992.
[52] S. Conlan, Y. Zhang, S. Cheley, H. Bayley, Biochemical and biophysical characterization of OmpG: a monomeric porin, Biochemistry 39 (2000) 11845–11854.
[53] J.E.W. Meyer, G.E. Schulz, Energy profile of maltooligosaccharide permeation through maltoporin as derived from the structure and from a statistical analysis of saccharide–protein interactions, Protein Sci. 6 (1997) 1084–1091.
[54] T. Schirmer, P.S. Phale, Brownian dynamics simulation of ion flow through porin channels, J. Mol. Biol. 294 (1999) 1159–1167.
[55] F. Dumas, R. Koebnik, M. Winterhalter, P. Van Gelder, Sugar transport through maltoporin of *Escherichia coli*, J. Biol. Chem. 275 (2000) 19747–19751.
[56] J.M. Rutz, J. Liu, A.J. Lyons, J. Goranson, S.K. Armstrong, M.A. McIntosh, J.B. Feix, P.E. Klebba, Formation of a gated channel by a ligand-specific transport protein in the bacterial outer membrane, Science 258 (1992) 471–475.
[57] R.A. Larsen, M.G. Thomas, K. Postle, Protonmotive force, ExbB and ligand-bound FepA drive conformational changes in TonB, Mol. Microbiol. 31 (1999) 1809–1824.
[58] S. Reumann, J. Davila-Aponte, K. Keegstra, The evolutionary origin of the protein-translocating channel of chloroplastic envelope membranes: identification of a cyanobacterial homolog, Proc. Natl. Acad. Sci. U. S. A. 96 (1999) 784–789.
[59] C.A. Mannella, On the structure and gating mechanism of the mitochondrial channel, VDAC, J. Bioenerg. Biomembranes 29 (1997) 525–531.
[60] K. Hill, K. Model, M.T. Ryan, K. Dietmeier, F. Martin, R. Wagner, N. Pfanner, Tom40 forms the hydrophilic channel of the mitochondrial import pore for preproteins, Nature 395 (1998) 516–521.
[61] R. Koebnik, Structural and functional roles of the surface-exposed loops of the β-barrel membrane protein OmpA from *Escherichia coli*, J. Bacteriol. 181 (1999) 3688–3694.
[62] S. Cheley, O. Braha, X. Lu, S. Conlan, H. Bayley, A functional protein pore with a "retro" transmembrane domain, Protein Sci. 8 (1999) 1257–1267.
[63] E. Sugawara, H. Nikaido, OmpA protein of *Escherichia coli* outer membrane occurs in open and closed channel forms, J. Biol. Chem. 269 (1994) 17981–17987.
[64] A. Arora, D. Rinehart, G. Szabo, L.K. Tamm, Refolded outer membrane protein A of *Escherichia coli* forms ion channels with two conductance states in planar lipid bilayers, J. Biol. Chem. 275 (2000) 1594–1600.
[65] N. Liu, A.H. Delcour, The spontaneous gating activity of OmpC porin is affected by mutations of a putative hydrogen bond network or of a salt bridge between the L3 loop and the barrel, Protein Eng. 11 (1998) 797–802.
[66] K. Saxena, V. Drosou, E. Maier, R. Benz, B. Ludwig, Ion selectivity reversal and induction of voltage-gating by site-directed mutations in the *Paracoccus denitrificans* porin, Biochemistry 38 (1999) 2206–2212.
[67] C.A. Mannella, Conformational changes in the mitochondrial channel protein, VDAC, and their functional implications, J. Struct. Biol. 121 (1998) 207–218.
[68] B. Schmid, L. Maveyraud, M. Krömer, G.E. Schulz, Porin mutants with new channel properties, Protein Sci. 7 (1998) 1603–1611.
[69] P. VanGelder, N. Saint, R. van Boxtel, J.P. Rosenbusch, J. Tommassen, Pore functioning of outer membrane protein PhoE of *Escherichia coli*: mutagenesis of the constriction loop L3, Protein Eng. 10 (1997) 699–706.
[70] D. Ulmke, J. Kreth, J.W. Lengeler, W. Welte, T. Schmid, Site-directed mutagenesis of loop L3 of sucrose porin ScrY leads to changes in substrate selectivity, J. Bacteriol. 181 (1999) 1920–1923.
[71] L.Q. Gu, O. Braha, S. Conlan, S. Cheley, H. Bayley, Stochastic sensing of organic analytes by a pore-forming protein containing a molecular adapter, Nature 398 (1999) 686–690.
[72] A. Kreusch, G.E. Schulz, Refined structure of the porin from *Rhodopseudomonas blastica*: comparison with the porin from *Rhodobacter capsulatus*, J. Mol. Biol. 243 (1994) 891–905.
[73] A.G. Murzin, A.M. Lesk, C. Chothia, Principles determining the structure of β-sheet barrels in proteins: I. A theoretical analysis, J. Mol. Biol. 236 (1994) 1369–1381.
[74] A.G. Murzin, A.M. Lesk, C. Chothia, Principles determining the structure of β-sheet barrels in proteins: II. The observed structures, J. Mol. Biol. 236 (1994) 1382–1400.
[75] W.M. Liu, Shear numbers of protein β-barrels: definition, refinements and statistics, J. Mol. Biol. 275 (1998) 541–545.